

# All-optical ultrafast control of beaming through a single sub-wavelength aperture in a metal film

Mohamed A. Swillam,\* Nir Rotenberg, and Henry M. van Driel

Department of Physics and Institute for Optical Sciences, University of Toronto, Toronto, M5S 1A7 Canada  
m.swillam@utoronto.ca

**Abstract:** We propose an ultrafast all-optical technique to control and beam the light emerging from a sub-wavelength slit in a planar gold film by exciting a transient grating in the area around the slit. A FDTD model is used to show how excitation of surface plasmon polaritons by the grating governs the beaming process. Both the grating and the beaming effect are shown to decay on a picosecond time-scale. An on-off contrast of 5 dB is obtained for the beaming, with a divergence angle of only 2.4 degrees.

©2011 Optical Society of America

**OCIS codes:** (240.6680) Surface plasmons; (250.5403) Plasmonics; (320.7080) Ultrafast devices; (320.7085) Ultrafast information processing.

---

## References and links

1. T. W. Ebbesen, H. J. Lezec, H. F. Ghaemi, T. Thio, and P. A. Wolff, "Extraordinary optical transmission through sub-wavelength hole arrays," *Nature* **391**(6668), 667–669 (1998).
2. H. J. Lezec, A. Degiron, E. Devaux, R. A. Linke, L. Martin-Moreno, F. J. Garcia-Vidal, and T. W. Ebbesen, "Beaming light from a subwavelength aperture," *Science* **297**(5582), 820–822 (2002).
3. F. J. García-Vidal, L. Martín-Moreno, H. J. Lezec, and T. W. Ebbesen, "Focusing light with subwavelength aperture flanked by surface corrugations," *Appl. Phys. Lett.* **83**(22), 4500–4502 (2003).
4. L. Martín-Moreno, F. J. García-Vidal, H. J. Lezec, A. Degiron, and T. W. Ebbesen, "Theory of highly directional emission from a single subwavelength aperture surrounded by surface corrugations," *Phys. Rev. Lett.* **90**(16), 167401 (2003).
5. F. J. García-Vidal, H. J. Lezec, T. W. Ebbesen, and L. Martín-Moreno, "Multiple paths to enhance optical transmission through a single subwavelength slit," *Phys. Rev. Lett.* **90**(21), 213901 (2003).
6. D. van Oosten, M. Spasenović, and L. Kuipers, "Nanohole chains for directional and localized surface plasmon excitation," *Nano Lett.* **10**(1), 286–290 (2010).
7. L. B. Yu, D. Z. Lin, Y. C. Chen, Y. C. Chang, K. T. Huang, J. W. Liaw, J. T. Yeh, J. M. Liu, C. S. Yeh, and C. K. Lee, "Physical origin of directional beaming emitted from a subwavelength slit," *Phys. Rev. B* **71**(4), 041405 (2005).
8. D. Z. Lin, C. K. Chang, Y. C. Chen, D. L. Yang, M. W. Lin, J. T. Yeh, J. M. Liu, C. H. Kuan, C. S. Yeh, and C. K. Lee, "Beaming light from a subwavelength metal slit surrounded by dielectric surface gratings," *Opt. Express* **14**(8), 3503–3511 (2006).
9. A. I. Fernández-Domínguez, E. Moreno, L. Martín-Moreno, and F. J. García-Vidal, "Beaming matter waves from a subwavelength aperture," *Phys. Rev. A* **74**(2), 021601 (2006).
10. C. T. Wang, C. L. Du, Y. G. Lv, and X. G. Luo, "Surface electromagnetic wave excitation and diffraction by subwavelength slit with periodically patterned metallic grooves," *Opt. Express* **14**(12), 5671–5681 (2006).
11. Z. Sun, "Beam splitting with a modified metallic nano-optic lens," *Appl. Phys. Lett.* **89**(26), 261119 (2006).
12. B. Guo, Q. Gan, G. Song, J. Gao, and L. Chen, "Numerical study of a high-resolution far-field scanning optical microscope via a surface plasmon-modulated light source," *J. Lightwave Technol.* **25**(3), 830–833 (2007).
13. N. Yu, Q. J. Wang, M. A. Kats, J. A. Fan, S. P. Khanna, L. Li, A. G. Davies, E. H. Linfield, and F. Capasso, "Designer spoof surface plasmon structures collimate terahertz laser beams," *Nat. Mater.* **9**(9), 730–735 (2010).
14. T. Ishi, J. Fujikata, K. Makita, T. Baba, and K. Ohashi, "Si nano-photodiode with a surface plasmon antenna," *Jpn. J. Appl. Phys.* **44**(12), L364–L366 (2005).
15. J. Christensen, A. I. Fernández-Domínguez, F. De Leon-Perez, L. Martín-Moreno, and F. J. García-Vidal, "Collimation of sound assisted by acoustic surface waves," *Nat. Phys.* **3**(12), 851–852 (2007).
16. H. A. Bethe, "Theory of diffraction by small holes," *Phys. Rev.* **66**(7-8), 163–182 (1944).
17. E. Hendry, F. J. García-Vidal, L. Martín-Moreno, J. G. Rivas, M. Bonn, A. P. Hibbins, and M. J. Lockyear, "Optical control over surface-plasmon-polariton-assisted THz transmission through a slit aperture," *Phys. Rev. Lett.* **100**(12), 123901 (2008).
18. N. Rotenberg, M. Betz, and H. M. van Driel, "Ultrafast all-optical coupling of light to surface plasmon polaritons on plain metal surfaces," *Phys. Rev. Lett.* **105**(1), 017402 (2010).
19. S. I. Anisimov, B. L. Kapeliovich, and T. L. Perelman, "Electron emission from metal surfaces exposed to ultrashort laser pulses," *Eksp. Teor. Fiz.* **66**, 776–781 (1974) (*Sov. Phys. JETP* **39**, 375 (1974)).

20. C.-K. Sun, F. Vallee, L. H. Acioli, E. P. Ippen, and J. G. Fujimoto, "Femtosecond-tunable measurement of electron thermalization in gold," *Phys. Rev. B* **50**, 15337 (1994).
21. K. S. Yee, "Numerical solution of initial boundary value problems involving Maxwell's equations in isotropic media," *IEEE Trans. Antenn. Propag.* **14**(3), 302–307 (1966).
22. A. Taflov, and S. C. Hagness, *Computational Electrodynamics: The Finite Difference Time Domain Method*, second edition (Artech House, Norwood, MA, 2000).
23. M. G. Moharam, E. B. Grann, D. A. Pommet, and T. K. Gaylord, "Formulation for stable and efficient implementation of the rigorous coupled-wave analysis of binary gratings," *J. Opt. Soc. Am. A* **12**(5), 1068–1076 (1995).
24. P. Lalanne, and G. M. Morris, "Highly improved convergence of the coupled-wave method for TM polarization," *J. Opt. Soc. Am. A* **13**(4), 779–784 (1996).
25. Z. Lin, and L. V. Zhigilei, "Thermal excitation of d band electrons in Au: implications for laser-induced phase transformations," **6261**, *Proc. SPIE 62610U* (2006).
26. J. Hohlfeld, S.-S. Wellershoff, J. Güdde, U. Conrad, V. Jähnke, and E. Matthias, "Electron and lattice dynamics following optical excitation of metals," *Chem. Phys.* **251**(1-3), 237–258 (2000).
27. R. Rosei, F. Antonangeli, and U. Grassano, "d Bands position and width in gold from very low temperature thermomodulation measurements," *Surf. Sci.* **37**, 689–699 (1973).
28. N. E. Christensen, and B. O. Seraphin, "Relativistic band calculation and the optical properties of gold," *Phys. Rev. B* **4**(10), 3321–3344 (1971).
29. R. D. Averitt, S. L. Westcott, and N. J. Halas, "Ultrafast optical properties of gold nanoshell," *J. Opt. Soc. Am. B* **16**(10), 1814 (1999).
30. N. Rotenberg, J. N. Caspers, and H. M. van Driel, "Tunable ultrafast control of plasmonic coupling to gold films," *Phys. Rev. B* **80**(24), 245420 (2009).
31. P. B. Johnson, and R. W. Christy, "Optical constants of the noble metals," *Phys. Rev. B* **6**(12), 4370–4379 (1972).
32. S. S. Akarca-Biyikli, I. Bulu, and E. Ozbay, "Resonant excitation of surface plasmons in one-dimensional metallic grating structures at microwave frequencies," *J. Opt. A, Pure Appl. Opt.* **7**(2), S159–S164 (2005).

## 1. Introduction

The manipulation of light using nanometallic structures has attracted considerable attention in the last decade [1-13]. The subwavelength control of optical and surface plasmon polariton (SPP) fields conferred by these structures leads to exciting applications such as extraordinary transmission [1], subwavelength focusing [2-8], and directional excitation or beaming [2-5]. In particular, a combination of metallic nanostructures with a periodic structure such as a grating have been proposed as the basis for beam-splitters [11], near and far field microscopes [12], small divergence angle laser sources [13], and light harvesting silicon photodetectors [14]. These structures have even been shown to enhance the beaming of classical waves, such as acoustic waves [15].

It is well known that light emerging from a sub-wavelength aperture is strongly diffracted [16]. Recently, it was experimentally demonstrated that the diffracted light could be beamed and controlled by surrounding the aperture with symmetric gratings [2]. Subsequently, there have been extensive experimental and theoretical studies of the characteristics of the light emerging from the aperture [3-5, 7-10]. The light beaming is due to the resonant excitation of SPPs on the aperture's outer surface, which then diffracts from the grating or the corrugated surface, and interferes with the light emerging from the slit. Consequently, the characteristics of the transmitted light are strongly dependent on the grating geometry. In particular, the angle at which the light is diffracted from or coupled to the grating determines the nature of the emergent beam [7,8]. Thus, the surrounding grating acts like an antenna that directs the beam. Conversely, these grating antennas can also be exploited to harvest the light impinging on the grating and collect it in the aperture region [14].

All the aforementioned designs and applications rely on the fabrication of either metallic or dielectric permanent gratings on a metal surface. Consequently, grating properties, such as the period or modulation depth, are static and cannot be readily controlled. Hence, these are effectively passive devices, with fixed transmittance characteristics. Control of the transmission from subwavelength apertures with surrounding gratings has recently been demonstrated using a photo-excited silicon grating [17]. The grating becomes metallic in the THz regime with the temporal recovery of this system limited by the carrier recombination time.

In this paper, we propose and model an ultrafast, all-optical method for the active control of visible light emerging from a subwavelength slit in a thin gold film. In essence, we adapt the transient thermal grating (TTG) technique in [18] to actively control beaming on a picosecond time scale. As shown in Fig. 1, two near-infrared femtosecond optical pulses are made to interfere in the gold and induce an electron temperature grating. Since the complex refractive index of gold is dependent on the free-electron temperature, a transient absorption and refraction grating results. The subsequent electron thermalization dynamics [18-20] control the beaming of a probe beam as it emerges from the aperture. This approach provides the basis for ultrafast switching and beaming applications.

The remainder of this paper is organized as follows. Section 2 briefly reviews the theoretical basis for the process whereby ultrashort light pulses can change the gold's electron temperature and consequently alter its complex refractive index. Section 3 outlines how these thermal effects can be used to generate a transient thermal grating (TTG). Finite-Difference Time-Domain (FDTD) [21, 22] and Rigorous Coupled Wave Analysis (RCWA) [23] are used to model diffraction from a grating on a plain metal film; these results are compared to previous experimental results to verify the theoretical models. In Section 4, the ultrafast beaming effect from a 50 nm thin gold film with a slit is simulated using the FDTD-based model. Finally, brief conclusions are offered in Section 5.

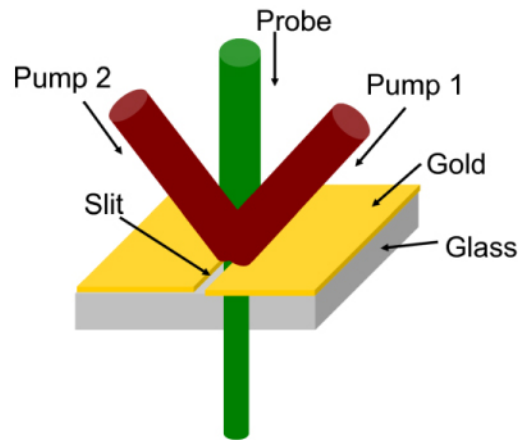


Fig. 1. Schematic diagram of a scheme to control light beaming.

## 2. The two temperature model for gold

The non-equilibrium, electron thermal dynamics induced by the interaction of a high intensity light pulse with a metal can be accurately described using the Two-Temperature Model [19-20, 24-26]. The two temperatures,  $T_{e,\ell}(z,t)$ , refer to that of the electrons ( $e$ ) and the lattice ( $\ell$ ) and are taken to be functions of time ( $t$ ) and depth into the sample ( $z$ ). Following earlier work [20, 26], we allow the excited electrons, not initially in a Fermi Dirac distribution, to possess a nonthermal energy density,  $N(z,t)$ , as well as the thermal energy density determined by a temperature. The dynamics of  $N$ ,  $T_e$  and  $T_\ell$  are then governed by a set of 3 coupled differential equations.

First, energy is instantaneously transferred from the laser pulse with power density  $P(z,t)$  to non-thermal electrons through linear absorption. The non-thermal energy density decays through electron-electron and electron-phonon collisions with time constants  $\tau_1$  and  $\tau_2$  respectively so that for a film of thickness  $d$

$$\frac{\partial N}{\partial t} = -\frac{N}{\tau_1} - \frac{N}{\tau_2} + P(z,t), \quad (1.1)$$

where

$$P(z, t) = \frac{(1-R)\alpha_{\text{eff}} I(t) e^{-\alpha_{\text{eff}} z}}{1 - e^{-\alpha_{\text{eff}} d}},$$

is the power density absorbed by the sample with  $I(t)$  being the time-dependent intensity of the beam, and  $R$  ( $\sim 0.96$  at 810 nm for a  $d = 50$  nm Au film) is the optical reflection coefficient. The quantity  $\alpha_{\text{eff}}^{-1}$  is the characteristic power deposition depth, which is the sum [26] of the characteristic optical absorption depth (15 nm for a wavelength of 810 nm) and the electron mean free path of the initially ballistic electrons; it has a value of  $\sim 100$  nm.

The time dependent electron temperature is governed by

$$C_e \frac{\partial T_e}{\partial t} = \frac{\partial}{\partial z} \left( K_e \frac{\partial T_e}{\partial z} \right) - g(T_e - T_\ell) + \frac{N}{\tau_1}, \quad (1.2)$$

where the first term on the right side describes the electron heat diffusion (negligible for a nearly uniformly illuminated thin film). The second term describes the equilibration between the electron and the lattice temperatures through a coupling constant  $g$ . The last term is the heating term which represents energy transferred from the non-thermal energy density to the thermalized electrons. Finally the time dependent lattice temperature is governed by

$$C_\ell \frac{\partial T_\ell}{\partial t} = g(T_e - T_\ell) + \frac{N}{\tau_2}. \quad (1.3)$$

The lattice thermalizes with the electrons after several picoseconds [20] and in general, the large value of  $C_\ell$  ensures that the gold lattice experiences only a small change in temperature; indeed, changes of hundreds of degrees to  $T_e$  lead to changes of only tens of degrees to  $T_\ell$ . Although, the cooling of the lattice is not contained in Eqs. (1), it depends on heat transfer to the substrate and typically occurs on a  $>100$  ps time scale. The coefficients in Eqs. (1.1)-(1.3) are given in Table 1.

The elevated electron temperature alters the complex dielectric constant or refractive index through changes in the occupancy of band states, by changing the electron distribution about the Fermi-energy and hence the available transitions [27, 28]. For visible light, the optical properties of gold are primarily determined by the  $d$ -band to conduction-band transitions, and the elevated temperature significantly alters the complex refractive index in the 520 to 570 nm wavelength region [27]. The use of this model has been validated by describing the optical properties of bulk gold [19,20, 25, 26], gold nano-particles [29] and the coupling of light to SPP via gratings [18,30].

We solve the 3 coupled differential equations numerically using the finite difference discretization of the differential equations; we use step sizes of 1.0 nm and 1.0 as in space and time, respectively, to ensure convergence of our solution.

**Table 1. Parameters Used in the TTM**

Symbol	Name	Value	Reference
$\tau_1$	Electron thermalization time	0.5 ps	[20]
$\tau_2$	Lattice thermalization time	1.0 ps	[20]
$C_e = \gamma T_e$	Electron heat capacity	( $\gamma$ ) $62.7 \text{ J m}^{-3} \text{ K}^{-2}$	[25]
$C_\ell$	Lattice heat capacity	$2.5 \times 10^6 \text{ J m}^{-3} \text{ K}^{-1}$	[25]
$K_e$	Electron thermal conductivity	$310 \text{ W m}^{-1} \text{ K}^{-1}$	[25]
$g$	Electron-phonon coupling constant	$2.2 \times 10^{16} \text{ W m}^{-3} \text{ K}^{-1}$	[25]

For the 50 nm gold film of this work, because of the large ballistic mean free path of the electrons the difference between the peak temperature at the front and back surface is < 1%. Consequently, in what follows we assume that the gold film can be accurately described by a uniform electron (and lattice) temperature.

### 3. Model for transient thermal grating

If now we have two pulses with time-dependent intensity  $I_1(t)$  and  $I_2(t)$  and they interfere along a given direction (taken to be the  $x$ -axis) on the gold surface, the resulting intensity is

$$I(x,t) = I_1(t) + I_2(t) + 2\sqrt{I_1(t)I_2(t)} \cos\left(\frac{2\pi}{\Lambda}x\right), \quad (2)$$

where  $\Lambda$  is the modulation period. This is given by

$$\Lambda = \frac{\lambda}{|\sin\theta_1 - \sin\theta_2|}, \quad (3)$$

where  $\lambda$  is the vacuum wavelength of the pump beams, and  $\theta_1$  and  $\theta_2$  are the incident angles of the two pump pulses.

From the intensity profile and the periodic boundary in the direction of the grating, we calculate the electron temperature grating in the gold. We then employ the model of Rosei *et al* [27] to translate the different electron temperatures into changes in the gold dielectric function. Lastly, we use this effective dielectric function in the FDTD simulations of the optical beaming effect (section 4). Where needed, we use the dielectric function of (the unheated) gold provided in [31].

The parameters used to calculate the transient change in the dielectric constant and model the optical beaming are the same as those used in [18] where, experimentally, it was demonstrated that an optically induced grating, as discussed above, could be used to couple light to SPPs on a planar gold film (without a slit). These parameters are: two 150 fs full-width at half-maximum (FWHM), 810 nm pulses that interfere on a 50 nm thick gold film. The angles of incidence and peak intensities of these beams are  $\theta_1 \sim 2^\circ$  and  $I_1 = 7.5 \text{ GW cm}^{-2}$  for pump 1, and  $\theta_2 \sim 43^\circ$  and  $I_2 = 5.3 \text{ GW cm}^{-2}$  for pump 2; this results in a 1200 nm period grating.

Before we model the optical beaming on a slotted film, to verify the validity of our approach we model the diffraction characteristics of the grating on a planar gold film without the slit, using both FDTD and RCWA. Figure 2 shows the simulation results for the undiffracted transmissivity,  $T^{(0)}$ , and first order diffraction transmissivity,  $T^{(-1)}$ , for both  $p$ - and  $s$ -polarized light, along with the corresponding experimental results from Ref. [18]; the agreement between the theory and the experiments is clearly evident.

In the experiments reported earlier [18], SPPs are coupled via the grating from a 450-750 nm white light continuum probe. The excitation of SPPs (see Fig. 2b) is confirmed by noting the difference in the  $p$ -polarized signal to an  $s$ -polarized signal. The zero-order spectra shown in Fig. 2b have a weak dependence on the wavelength as the grating and thermal effects are small. In contrast, the first-order diffraction, shown in Fig. 2a, is strongly dependent on the induced changes to the dielectric function of the gold, and varies by an order of magnitude over the same spectral range. From the difference between the  $s$ - and  $p$ -polarization cases in Fig. 2b we calculate that the total plasmonic coupling efficiency for the experiment/simulations is 0.018 at a wavelength of 560 nm.

The temporal dynamics of the grating, and the plasmonic coupling, are as follows [18]: A peak temperature contrast between the hot and the cold regions of the grating, and hence a maximum diffraction and coupling efficiency, is reached  $\sim 0.6$  ps after the pump-probe overlap. At this time, the energy content of the hot electrons is at a maximum, with the electrons thermalized but with only a small amount of energy transfer to the lattice. The

grating then decays as electron energy is lost to the lattice and hence the plasmonic coupling decays with a time constant  $< 1$  ps.

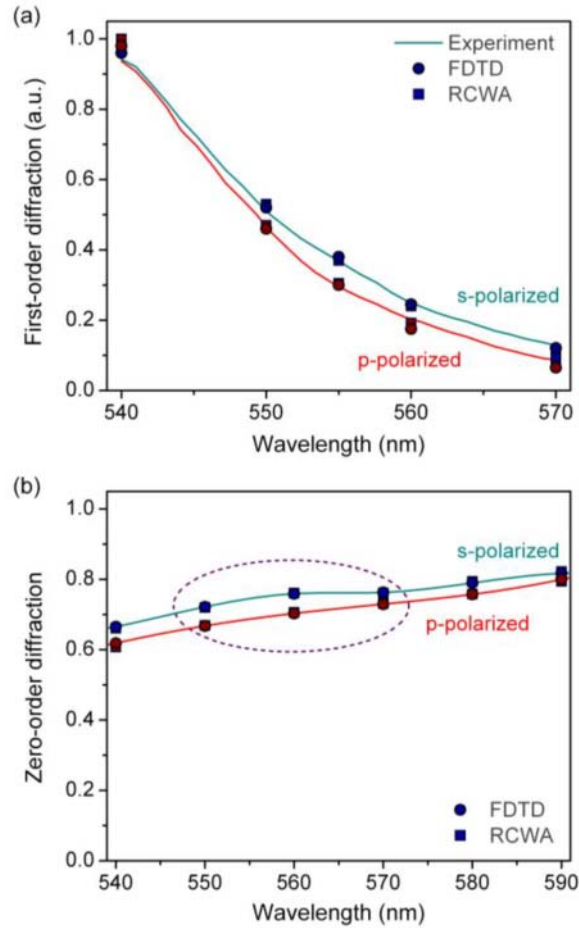


Fig. 2. (a) The first-order and (b) zero-order diffraction spectra for the TTG experiment, at the delay time corresponding to the peak pump-induced grating. In (a) the curves are the experimental results, taken from Ref. 18, while in (b) they are guides to the eye. In both parts the results of the FDTD calculations are shown as circles, while those of the RCWA calculations are shown as squares. In (b), the spectral region where plasmonic coupling occurs is circled.

#### 4. Transient beaming effect

As shown in the last section, the FDTD technique can accurately model the experimental diffraction and SPP coupling effects from a transient grating. From the Helmholtz reciprocity theorem we expect that a grating that couples light to a SPP can also diffract light from the SPP [7,8] and consequently we should be able to employ our model to characterize the situation shown in Fig. 1, in which we expect beaming to occur on ultrafast time-scales. Since the dynamics of the beaming depend on those of the grating, we expect a beaming window that closes in  $\sim 1.0$  ps.

In Fig. 3 we show the results of FDTD simulations for a continuous 560 nm probe that impinges on a 50 nm gold film with a 100 nm slit, for different time-steps. A 1.0 nm square grid cell is utilized. In the sub-plots we show the intensity of the light emerging from the slit (at the bottom) for different time delays, relative to the arrival of the pump pulse; for clarity,

the intensity in all sub-plots are normalized to the maximum intensity present for  $p$ -polarized light at the time delay corresponding to the highest contrast grating (Fig. 3d).

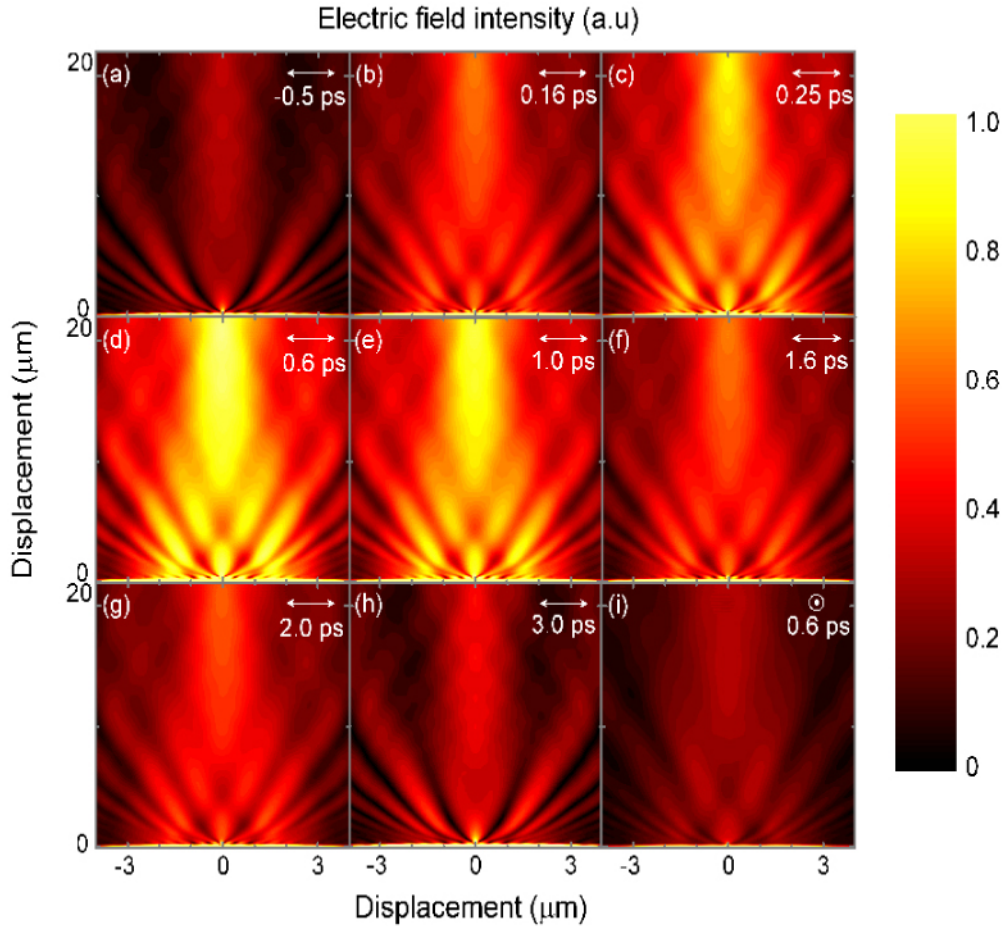


Fig. 3. (Media 1) The spatial distribution of the electric field intensity of the light that is transmitted through a sub-wavelength slit (located at the bottom, at 0 on the horizontal scale) in a 50 nm thick gold film, for different delay times. The polarization of the light is shown in the upper right corner of each figure: (a) to (h) are for  $p$ -polarized light, while (i) is for  $s$ -polarized light and is shown for the same delay time as in (d). All figures are normalized such that a value of 1 corresponds to the highest intensity in (d).

The dynamics of the beaming are clearly seen in Figs. 3(a-h) for a  $p$ -polarized probe. Shortly before overlap (a) very little beaming is seen. Then, as more energy is absorbed by the gold and the grating contrast is increased, so too does the magnitude of the beaming, as is seen near the center of (b) and (c); this beaming is maximal at  $t = 0.6$  ps (d). Subsequently, as the grating decays, so too does the amount of beaming that occurs (e-h). Clearly, the beaming is dependent on the presence of the grating.

We attribute this beaming to the resonant excitation of SPPs on both surfaces of the film by the TTG. We verify this by repeating the FDTD calculations at  $t = 0.6$  ps, this time for  $s$ -polarized light (i). Here we observe no beaming, in comparison with Fig. 3d, supporting our hypothesis. We further confirm the presence of SPPs by zooming in on the area immediately surrounding the slit, for  $t = 0.6$  ps, and for both polarizations (Fig. 4). Again, the SPPs are seen as modulations of the electric field on both sides of the gold film for the  $p$ -polarized light (Fig. 4a), but they are absent for  $s$ -polarized light (Fig. 4b). Consequently, it is evident that the

beaming is caused by the TTG, which couples light to SPPs both enhancing and beaming the transmitted light.

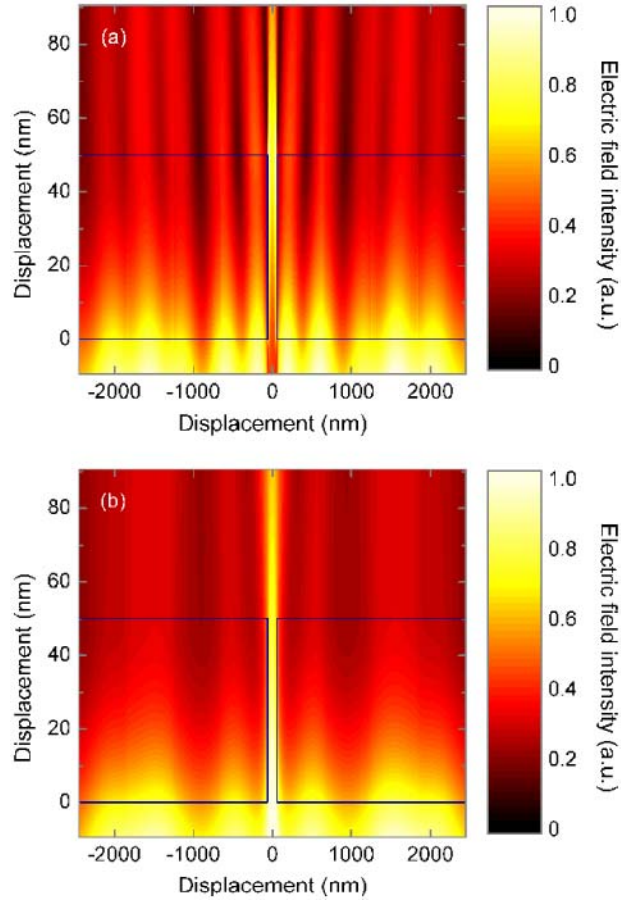


Fig. 4. The electric field intensity in the area immediately surrounding the slit for both (a) *p*-polarized and (b) *s*-polarized excitations. The gold film and the slit are shown in blue lines. The plots are normalized in the same manner as Fig. 3.

To better study both the spatial behavior and the dynamics of the beaming we show the spatial distribution of the electric field intensity at the distance of  $20\ \mu\text{m}$  away from the slit, for select delay times, in Fig. 5. For a time delay of  $0.6\ \text{ps}$  the main peak of the intensity profile has a FWHM of  $1.75\ \mu\text{m}$ , corresponding to a divergence angle of  $2.4$  degrees; this value is comparable to, but slightly smaller than, that reported previously [2].

We show the maximum intensity at a distance of  $20\ \mu\text{m}$  from the slit as a function of the time delay in the inset to Fig. 5. Due to the TTG, the peak intensity rises from a background value of  $0.31$  to  $1.0$ , an increase by a factor of  $\sim 3$ ; recall that this increase occurs in  $\sim 0.6\ \text{ps}$ . We extract an exponential decay constant from this inset of  $1.2 \pm 0.2\ \text{ps}$ , demonstrating that the beaming window is indeed ultrafast.

While the enhancement of the beaming that we observe is slightly higher than the one recently reported in the THz regime [17], it is lower than that reported with the use of surface relief gratings. In particular, enhancements of the beaming by factors ranging from  $7$  to  $15$  have been reported, using double-sided metal gratings [5, 32]. Of course, in these cases there is no active control of the emergent beam; in essence, since the plasmonic coupling is mediated in an all-optical fashion, rather than with a static scheme, the overall efficiency of the beaming is decreased, but it can now be manipulated on ultrafast time-scales.

The enhancement of the beaming process can be optimized in different ways, such as by increasing the change to the dielectric constant of the gold. This can be done by increasing the temperature of the electrons in the metal film either by using higher pump fluence, by using thinner films, or by increasing the length of the pump pulse. In particular, increasing the pulse length would also lengthen the time during which beaming occurs.

We note that our scheme for the active control of beaming is both tunable and broadband. TTG have been shown to resonantly excite plasmons across a broad band of wavelengths,

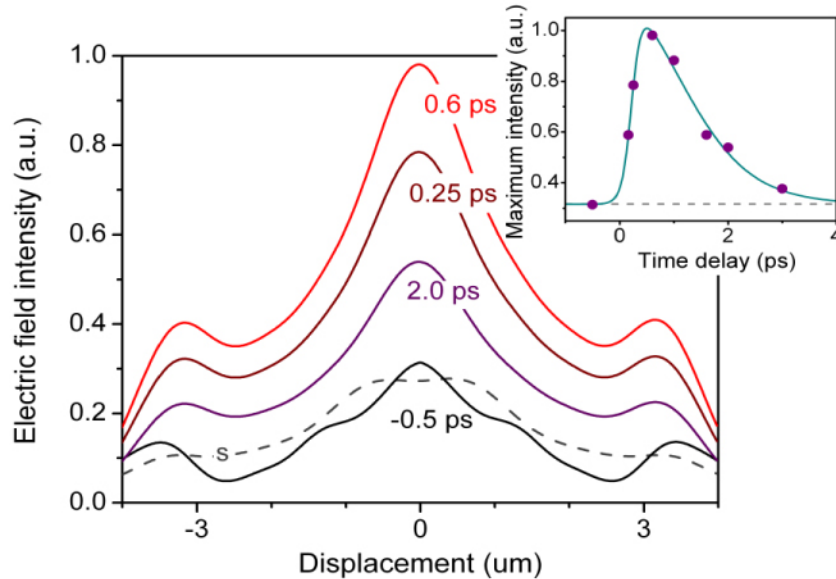


Fig. 5. The spatial distribution of the *p*-polarized electric field intensity at a distance of 20  $\mu\text{m}$  from the slit, for different delay times. The *s*-polarized intensity for  $t = 0.6$  ps is shown as a dashed curve. The inset shows the maximum intensity present at each delay time (corresponding to Fig. 3); the curve is a guide to the eye.

ranging from 520 to 570 nm [18]. Consequently we expect the current scheme to operate in the same range of wavelengths, albeit with decreasing efficiency both as the wavelength increases and the pump-induced changes to the dielectric function of the gold decrease [27], and as the wavelength becomes resonant with the *d*-band transition at 520 nm and energy is lost to the gold instead of coupling to a SPP. It is important to note that a change in the wavelength at which beaming occurs necessitates a change in grating period, as the angle at which the light diffracts must be optimized.

## 5. Conclusions

In summary, ultrafast beaming of the light emerging from a sub-wavelength aperture in planer metal film is demonstrated using FDTD simulations. We show an on-off contrast of 4.95 dB and that the system recovers within  $\sim 1.0$  ps. The beaming effect is controlled optically using the linear absorption of a pump pulse that creates a transient grating on the metal surface. Simulations reveal that the grating-assisted coupling of light to SPPs on the metal is the dominant mechanism for the beaming. This type of ultrafast all-optical control can form the basis for future optical and plasmonic switches.

## Acknowledgements

The authors gratefully acknowledge funding from the Natural Sciences and Research Council of Canada.